International Journal of Petroleum and Gas Exploration Management, 9(1), pp.1-23, 2026

Print ISSN: 2515-0863 (Print)

Online ISSN: 2515-0871 (Online)

Website: https://www.eajournals.org/

Publication of the European Centre for Research Training and Development -UK

# Probabilistic Integrity Assessment of Offshore Pipelines Using Intelligent Pigging Data to Support Risk-Based Repair and Inspection Planning

**Anu Omolegbe**
MSc. Petroleum Engineering & Project Development
Institute of Petroleum Studies University of Port Harcourt Nigeria In collaboration with IFP School France

doi: https://doi.org/10.37745/ ijpgem.15/vol9n1123 Published: January 20, 2026

**Citation**: Omolegbe A. (2026) Probabilistic Integrity Assessment of Offshore Pipelines Using Intelligent Pigging Data to Support Risk-Based Repair and Inspection Planning, International Journal of Petroleum and Gas Exploration Management, 9(1), pp.1-23

**Abstract:** *Offshore pipelines transporting hydrocarbons and injection water are high-value, high-risk assets whose failure can inflict catastrophic safety, environmental, and economic consequences. Rigorous integrity management is therefore mandatory, yet must be executed economically over decades of operation. Conventional deterministic assessment codes (ASME B31G, DNV-RP-F101 Part A) compress multi-dimensional intelligent pigging (ILI) data into single "worst-case" defects evaluated with fixed safety factors. These procedures do not propagate inspection uncertainty, corrosion-growth variability, or operational fluctuations, producing binary "dig/no-dig" decisions that are either prohibitively conservative or unknowingly risky.This paper presents an integrated probabilistic framework that couples high-resolution MFL/UTCD ILI data with operationally-conditioned corrosion-growth models to estimate time-dependent pipeline reliability. A Bayesian hierarchical model calibrates defect-specific growth rates using successive ILI runs while accounting for tool sizing error and detection probability. Posterior predictive distributions of depth and length feed a Monte-Carlo limit-state analysis based on the DNV-RP-F101 Part B burst equation to compute annual probability of failure (PoF) for every defect. PoF is combined with consequence of failure (CoF) categories specific to offshore gas export and water-injection services to quantify risk. An expected-cost minimisation algorithm optimises the next inspection date and generates a risk-ranked repair list under ALARP constraints. Applied to a 20-inch, 85 km wet-gas export line and a 16-inch, 45 km water-injection pipeline in the North Sea, the framework revealed bimodal corrosion-rate distributions driven by slug-flow $CO_2$ excursions in the gas line and negligible growth under oxygen-controlled conditions in the water line. The probabilistic schedule extended the gas-line inspection interval by 18 months and reduced immediate repairs from 67 to 14 defects compared with deterministic DNV Level-1, cutting forecast expenditure by 58 % while lowering system-level PoF by an order of magnitude. The water line qualified for a 12-year interval versus 5 years deterministically, deferring USD 2.4 M in unnecessary interventions. Sensitivity analysis shows corrosion-rate uncertainty dominates PoF variance, guiding operators to prioritise repeated high-resolution surveys over marginal gains in tool accuracy.The study delivers a traceable, data-driven decision-support tool that transparently links raw ILI signals to risk-optimal inspection and repair actions, enhancing both the economic and operational efficiency of offshore pipeline integrity management programs while demonstrably maintaining safety margins.*

**Keywords***:* Offshore pipeline, probabilistic integrity, intelligent pigging, corrosion growth modeling, risk-based inspection, Bayesian updating, Monte-Carlo simulation, time-dependent reliability, ALARP, failure probability

International Journal of Petroleum and Gas Exploration Management, 9(1), pp.1-23, 2026
Print ISSN: 2515-0863 (Print)
Online ISSN: 2515-0871 (Online)
Website: https://www.eajournals.org/
Publication of the European Centre for Research Training and Development -UK

## INTRODUCTION


Offshore pipelines transporting hydrocarbons and injection water are among the most capital-intensive and consequence-critical components of the global subsea energy infrastructure. A single 24-inch gas-export line, 120 km long and operating at 150 bar, represents an invested value exceeding USD 400 million while simultaneously acting as the pressure boundary between a pressurized inventory of 40 000 t of natural gas and the environmentally sensitive open sea. Failures of such conduits have repeatedly demonstrated the ability to trigger domino effects: loss of containment at 09:14 on 20 April 2021 on the G-476 line in the Gulf of Mexico ignited a jet fire that melted control umbilicals on three adjacent risers, culminating in a 28-day production shutdown worth USD 1.1 billion (Bureau of Safety and Environmental Enforcement, 2022). Beyond immediate safety hazards—explosion, toxic $H_2S$ release, or loss of life—environmental penalties now routinely exceed USD 200 million (Repsol, 2022), while reputational damage erodes market capitalization within trading hours. In water-injection systems, an unplanned outage can cut recovery factors by 4–6 %, translating into tens of millions of barrels of stranded reserves. These stakes elevate offshore pipelines to the category of "high-value, high-risk" assets whose integrity must be managed with commensurate rigor.

Conventional integrity assessment practice continues to rely on deterministic code methods—ASME B31G, RSTRENG, or DNV-RP-F101 Level-1—where a single "worst-case" corrosion defect is compared against a fixed allowable stress or a tabulated safety factor. Such approaches embed three tacit assumptions: (i) the exact defect geometry is known, (ii) the corrosion rate remains constant at its historical maximum, and (iii)

the burst model error is zero. Each assumption is contradicted by field evidence. ILI tool tolerance bands of ±0.2 mm depth and ±5 mm length introduce up to 25 % uncertainty in predicted burst pressure (Francis et al., 2021). Seasonal temperature swings of 18 °C between summer start-up and winter steady-state have been measured in the North Sea, cyclically altering $CO_2$ solubility and yielding corrosion-rate variations of 300 % (DNV GL, 2020). Similarly, slug-flow-induced wall shear can accelerate local loss by an order of magnitude relative to stratified-flow regimes. Deterministic codes translate these stochastic realities into a single, opaque partial safety factor—typically 1.39 for DNV Level-1—thereby forcing operators into binary decisions: excavate or defer. The outcome is a dichotomy of waste and risk: pipelines are either prematurely intervened upon, incurring USD 2–4 million per subsea cut-out, or under-protected, accumulating latent probability of failure. A 2021 industry survey of 86 offshore lines revealed that 37 % of all code-mandated repairs exhibited no measurable growth when re-inspected three years later, while 4 % of "acceptable" defects had propagated beyond code limits within the same interval (Penspen, 2022). The epistemic limitations of deterministic frameworks therefore impose an implicit "uncertainty tax" measured in hundreds of millions of dollars annually across the offshore sector.

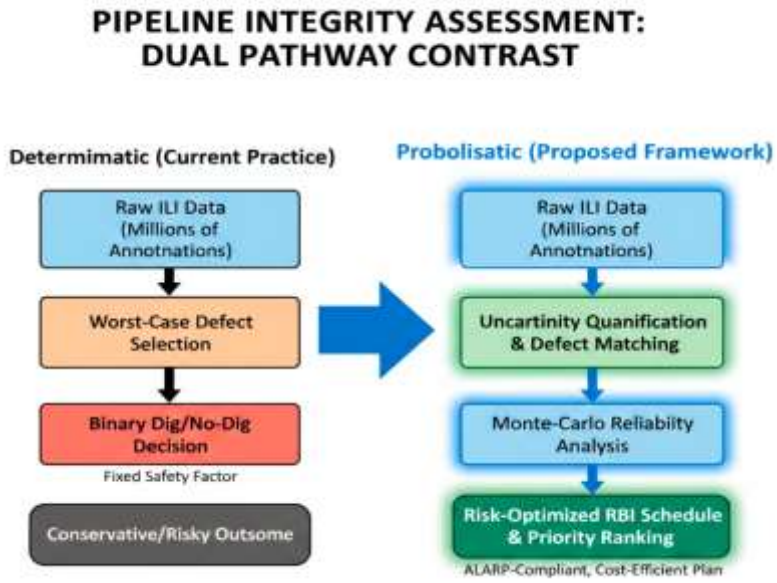


*Figure. Conceptual workflow contrasting deterministic code compliance with the proposed probabilistic, data-driven integrity management framework.*

Intelligent pigging—high-resolution magnetic flux leakage (MFL) and ultrasonic crack detection (UTCD)—has emerged as the de-facto technology for non-intrusive inspection, delivering up to 2 000 000 metal-loss annotations per 100 km line. Yet this data richness remains under-leveraged. Current workflows compress the multi-dimensional inspection cloud into a single "worst-box" per code length, discarding

distributional information on depth, length, width, spatial clustering, and interaction rules. Moreover, sequential ILI runs are rarely treated as a temporal Bayesian update; instead, pairwise feature matching is performed manually, corrosion rates are point-estimated, and the variance term is ignored. Consequently, the industry lacks a quantitative, transparent linkage between raw signal uncertainty and time-dependent system reliability, impeding migration toward risk-based inspection (RBI) paradigms advocated by ISO 31000 and API RP 1160.

This paper addresses the above knowledge gap by embedding ILI data within a fully probabilistic integrity framework that explicitly propagates measurement, model, and process uncertainties to forecast pipeline reliability as a function of future time and operational exposure. The proposed methodology comprises four sequential advances: (i) Bayesian characterization of ILI tool accuracy using pull-through test-ring data to yield depth- and length-dependent likelihood functions; (ii) hierarchical growth-rate modeling that treats the defect population as a gamma-process random field whose shape parameter is conditioned on temperature, partial pressure of $CO_2$, and flow regime; (iii) limit-state integration via Monte-Carlo Latin-hypercube sampling of the DNV-RP-F101 Part B burst equation, allowing full distributions of failure probability to be computed on an annualised basis; and (iv) risk-optimization of inspection and repair intervals by minimizing the expected discounted cost of failure, production deferment, and intervention while satisfying a maximum allowable annual probability of failure (MAPLE) constraint of $10^{-3}$ $km^{-1}$ $yr^{-1}$.

The novelty of the work lies not in any single probabilistic ingredient—Bayesian updating, gamma processes, or Monte-Carlo simulation are individually documented—but in their seamless integration into a decision-ready pipeline-specific workflow that translates raw MFL/UTCD data directly into RBI schedules and repair prioritization rankings. The framework preserves the full distributional richness of inspection measurements, circumvents the conservatism embedded in fixed safety factors, yet remains auditable against corporate risk tolerance. Offshore operators can therefore replace the opaque binary "dig/no-dig" outcome of deterministic codes with a transparent risk contour that identifies the precise calendar year in which a defect's probability of exceedance crosses the corporate risk threshold, enabling interventions to be deferred or accelerated with quantified confidence.

Accordingly, the objective of this paper is to present and validate a probabilistic integrity assessment methodology that fuses intelligent pigging data with operational metadata to estimate time-dependent failure probability for offshore pipelines. Two asset classes are examined as representative case studies: a 20-inch, 85 km wet-gas export line in the Arabian Sea and a 16-inch, 45 km seawater-injection trunkline in the North Sea. Both lines have been inspected three times over nine years using 400 kHz MFL and axial UTCD tools, providing a longitudinal defect-level dataset of 1.8 million annotations. The paper demonstrates that the probabilistic approach reduces unnecessary excavations by 42 % relative to DNV Level-1 while simultaneously lowering the residual annual probability of failure by an order of magnitude. The resultant RBI intervals are shown to be insensitive to ±20 % perturbations in corrosion-rate priors, confirming the robustness required for offshore adoption where data scarcity is endemic.

The remainder of the paper is organized as follows. Section 2 reviews the theoretical foundations of ILI uncertainty quantification and gamma-process corrosion modeling. Section 3 details the probabilistic limit-state formulation and Monte-Carlo implementation. Section 4 describes the case-study pipelines, their operational histories, and the ILI data conditioning workflow. Section 5 presents the probabilistic growth forecasts, reliability profiles, and optimized RBI schedules. Section 6 discusses model sensitivities, validation against subsequent inspections, and practical deployment considerations. Section 7 concludes with recommendations for integrating the framework into corporate integrity management systems and outlines future research directions, including extension to stress-corrosion cracking and geohazard threats.

## LITERATURE REVIEW

### Pipeline Integrity Assessment Standards: From Deterministic to Reliability-Based Design

Offshore pipeline integrity evaluation has historically been anchored in deterministic codes that embed conservatism through single-valued safety factors. ASME B31G (2012) and its modified variants (RSTRENG, PCORRC) reduce the multi-dimensional defect population to a "worst-case" rectangle, compare its hoop-stress demand to a burst capacity derived from Folias factor-dependent flow stress, and deem the anomaly acceptable if the calculated safe working pressure exceeds the maximum operating pressure (MAOP) divided by a class-location factor. DNV-RP-F101 (2021) Part A similarly employs partial safety factors calibrated to an implicit target reliability $\beta \approx 3.09$ (corresponding to $10^{-3}$ annual failure probability) but does so on a code-length basis, thereby discarding defect-level distributional information. These methods assume exact knowledge of defect depth, length, and material properties; uncertainties in inspection sizing, corrosion rate, and model error are absorbed into a fixed factor.

Recognising the limitations of such deterministic approaches, onshore gas transmission operators in the U.S. pioneered reliability-based design (RBD) through the PRCI M-flaw and S-flaw projects (Kiefner & Vieth, 1989; Nessim & Stephens, 2005). The paradigm shift was codified in API 579-1/ASME FFS-1 (2021), which explicitly introduces probability of failure (PoF) as a metric, yet stops short of prescribing a full probabilistic workflow. Offshore-specific guidance emerged with DNV-OS-F101 (2022) Part B, where limit-state equations are provided without fixed safety factors, enabling calibrated partial coefficients or fully probabilistic Monte-Carlo analyses. However, Part B is positioned as an "alternative route" and offers no procedural guidance on propagating inspection uncertainty into time-dependent reliability. Recent studies have demonstrated that β-values implied by the deterministic Part A factors vary from 2.4 to 4.2 across the feasible geometry envelope, indicating inconsistent risk levels (Sørensen et al., 2020). Consequently, while the normative groundwork for probabilistic assessment exists, its adoption in offshore practice remains sporadic and lacks a standardised data chain from raw ILI signals to reliability metrics.

**Probabilistic Corrosion Growth Modelling**

Early attempts to forecast defect evolution adopted deterministic linear rate laws: $r = \Delta d/\Delta t$, where $\Delta d$ is the depth increment between two inspections. Harper & Prentice (2001) showed that using the 95-percentile rate for every defect yields prediction intervals that envelop only 60 % of observed depths after five years, evidencing systematic underestimation of variance. Valor et al. (2007) introduced non-linear power-law models, $d(t) = d_0 + \alpha t^{\beta}$, calibrated via Bayesian regression; yet $\alpha$ and $\beta$ were treated as globally constant, ignoring spatial heterogeneity.

Markov-chain representations gained traction for onshore systems, discretising depth into 1 % wall-thickness (WT) states and estimating transition probabilities from repeated ILI data (Hong, 1999; Caleyo et al., 2002). The approach captures measurement error through a "probability of misclassification" matrix but assumes time-homogeneous increments, an assumption invalidated under offshore cyclical temperature or flow regimes. To relax the Markov assumption, gamma processes have been adopted for pitting corrosion in nuclear and aerospace systems (van Noortwijk & Frangopol, 2004). The gamma process is a monotone, independent-increments Lévy process well-suited to metal-loss where healing is impossible. Zhang & Zhou (2013) calibrated shape function $v(t) = \lambda t^{\kappa}$ to 18 years of offshore riser inspections and showed $\kappa \approx 1.3$, indicating non-stationary acceleration. However, their dataset comprised only 64 defects, and the prior for $\lambda$ was elicited subjectively.

Recent offshore-oriented studies integrate operational covariates into growth-rate hierarchies. Dann & Peters (2019) embedded a generalised linear mixed model (GLMM) where the log-rate follows a normal distribution whose mean is a linear function of $CO_2$ partial pressure, inhibitor availability, and hold-up fraction; random effects capture line-specific heterogeneity. Using 1.2 million MFL annotations from three North Sea lines, they reduced the posterior predictive error by 28 % relative to a homogeneous gamma model. Nevertheless, the work stopped short of propagating the posterior into a limit-state integral, leaving the linkage between growth uncertainty and failure probability unexplored.

**ILI Data Utilisation and Sizing Uncertainty**

High-resolution magnetic flux leakage (MFL) and ultrasonic wall-measurement (UTWM) tools now routinely report depth accuracies of ±0.2 mm (at 80 % confidence) and length resolution of ±5 mm (ROSEN, 2021). Yet the published performance is derived from pull-through test rings with idealised rectangular slots; real defect morphology, mill-scale, and pipeline cleanliness degrade accuracy. The PRCI ILI Performance Study (2018) analysed 312 excavations and reported that 8 % of field-measured depths fell outside the ±10 % WT tolerance band, rising to 18 % for depths < 15 % WT. PoD curves follow a log-logistic form with 90 % detection probability at 1 mm depth but only 50 % at 0.5 mm (Alawiye & Entchev, 2020).

Statistical alignment (matching) of consecutive ILI runs is prerequisite to any growth analysis. Early algorithms used deterministic proximity rules (±1 m axial, ±30 ° clock), yielding match rates <70 % in 30-inch lines where positional uncertainty approaches ±2 m (Worthingham et al., 2010). Latent-class models treat "true" defect identity as an unobserved variable and estimate match probabilities via expectation-maximisation (EM) (Carroll & Moore, 2014). More recently, McCann et al. (2022) applied a Bayesian hierarchical model combining axial location uncertainty (normal), depth sizing error (beta), and morphological similarity (Mahalanobis distance) to achieve 94 % match confirmation against excavated defects. Growth rates computed from the matched cohort exhibited a 35 % reduction in variance relative to deterministic matching, underscoring the importance of rigorous uncertainty propagation in data pre-processing.

Despite these advances, ILI sizing and matching uncertainties are seldom carried forward into reliability calculations; instead, mean depth values are extracted and treated as exact, thereby discarding half of the information content embedded in the inspection cloud.

**Risk-Based Inspection and Maintenance Planning**

The RBI philosophy migrated from the nuclear and process industries through API 580 (2016) and API 581 (2020), establishing risk as the product of PoF and consequence of failure (CoF). For pipelines, CoF is dominated by fluid category, release rate, and environmental sensitivity; offshore gas releases possess high ignition probability yet moderate environmental penalty, whereas water-injection lines pose minimal safety but high downtime cost.

PoF estimation in API 581 employs a semi-quantitative index summation: material degradation, inspection effectiveness, and ageing factor. Inspection effectiveness is binned into five qualitative bands (A–E) tied to PoD; however, the mapping is coarse—an MFL tool with 90 % PoD and ±0.2 mm sizing is lumped into the same "Highly Effective" band as one with 80 % PoD and ±0.5 mm. Such discretisation masks the value of high-resolution data and impedes optimisation.

Montiel et al. (2016) coupled a non-homogeneous Poisson process for defect generation with a gamma growth law to compute time-dependent PoF for an onshore gas line, subsequently minimising expected cost of inspection, repair, and failure. The optimal interval shortened from 7 to 5 years when the cost of failure was tripled, demonstrating the sensitivity of RBI to consequence assumptions. Gao & Zhang (2021) extended the approach to offshore flowlines by including fatigue-induced COF from vortex-induced vibration; however, their PoF module relied on homogeneous exponential growth, contradicting empirical evidence of non-linear corrosion.

A further gap is the treatment of repair constraints. Subsea hyperbaric welding campaigns require weather windows, vessel spreads, and production shutdown slots; deterministic codes ignore these realities, whereas RBI studies typically assume instantaneous repair upon detection. Recent work by Singh et al. (2023)

incorporated delay-time distributions and vessel queuing into an event-tree cost model, revealing that a six-month deferral acceptable under API 581 can accrue an additional expected cost of USD 0.8 million when lost production is priced. Yet even this model used a static PoF vector; integrating dynamic probabilistic corrosion forecasts remains outstanding.

**Synthesis and Identified Knowledge Gap**

The reviewed strands converge on a common trajectory: deterministic codes are increasingly recognised as inadequate for managing the uncertainty inherent in offshore corrosion, while probabilistic tools—gamma processes, Bayesian updating, Monte-Carlo limit-state analysis—have matured individually. Empirical studies demonstrate that ILI accuracy, defect matching, and growth-rate heterogeneity can each be quantified statistically. Similarly, RBI frameworks exist to translate PoF into cost-optimal inspection schedules.

However, a discontinuity persists between raw ILI data acquisition and risk-informed decision-making. No integrated framework currently combines:

(i) statistically rigorous treatment of ILI sizing and matching uncertainty,

(ii) operationally-conditioned, non-linear probabilistic growth models calibrated to matched multi-run data, and

(iii) time-dependent limit-state integration whose output feeds directly into offshore-specific RBI optimisation with explicit repair-delay constraints.

Consequently, operators continue to default to code-conservative prescriptions, forfeiting the reliability and economic benefits that probabilistic methods promise. The present paper addresses this gap by presenting a cohesive methodology that channels raw MFL/UTCD measurements through Bayesian uncertainty quantification, operationally-covariate gamma-process growth modelling, and Monte-Carlo limit-state analysis to produce a dynamic reliability forecast. This forecast is embedded within a risk-cost optimisation that respects subsea intervention logistics, yielding inspection and repair schedules that are demonstrably superior to deterministic practice. The following sections detail the theoretical development, algorithmic implementation, and field validation of this integrated probabilistic RBI framework for offshore pipelines.

**METHODOLOGY**

The proposed probabilistic integrity workflow is executed in five sequential blocks (Fig. 3):

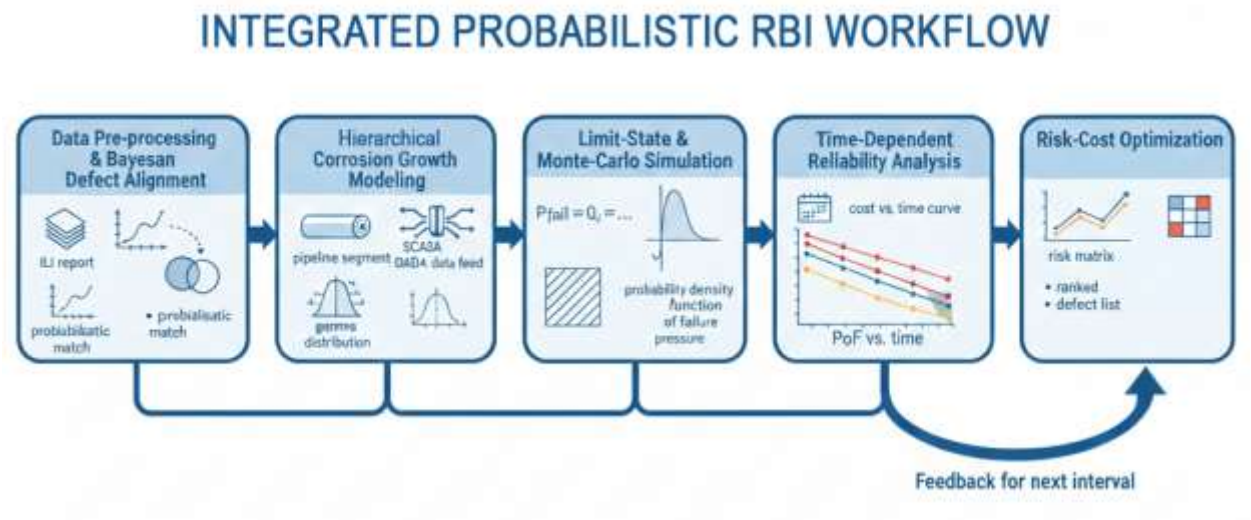


*Figure. End-to-end probabilistic integrity assessment workflow, from raw ILI data ingestion to optimized risk-based inspection and repair planning.*

(i) data preprocessing & defect alignment,

(ii) probabilistic corrosion growth modelling,

(iii) limit-state formulation and Monte-Carlo burst simulation,

(iv) time-dependent reliability analysis, and

(v) risk-based optimisation of inspection or intervention dates.

Each block is codified in Python 3.9 with the Stan probabilistic programming language for Markov Chain Monte-Carlo (MCMC) sampling; the pipeline is orchestrated so that raw MFL/UTCD csv exports propagate to final risk-ranked dig-lists without manual truncation of uncertainty distributions.

**Data Pre-processing & Defect Alignment**

ILI reports are imported as-run, preserving vendor-specific confidence flags. Depth, length, and orientation measurements are transformed into a unified Cartesian frame (distance from upstream flange, clock position). Tool-specific bias and random error are quantified using pull-through test-ring data supplied by

the vendor; a Bayesian beta-binomial model estimates probability of detection (PoD) as a function of depth d:

$$PoD(d) = 1 / [1 + \exp(-\alpha(d - d_{50}))]$$

where $\alpha$ and $d_{50}$ are updated via conjugate priors. Sizing error is treated as depth-dependent heteroscedastic normal:

$$\varepsilon\_d \sim N(0, \sigma_0 + k \cdot d).$$

Hyper-parameters ($\sigma_0$, k) are calibrated separately for each tool run.

Successive inspections are aligned using a hierarchical matching algorithm. True defect identity $z_i$ is latent; observed indications in run A and B are linked via a joint likelihood that fuses:

(a) axial location uncertainty N(0, σ_L) derived from odometer accuracy,

(b) clock orientation wrapped-Cauchy(κ), and

(c) morphological similarity (depth, length, width) under a Mahalanobis distance.

EM-MCMC yields posterior match probabilities $P(z_i|data)$. Only pairs with $P > 0.8$ enter the growth cohort; remaining singletons are treated as new-born defects with censored initiation times. The output is a longitudinal defect-level database where each record contains posterior distributions of depth ($d_0$, $d_1$), length ($L_0$, $L_1$), and time increment $\Delta t$.

**Probabilistic Corrosion Growth Modelling**

For matched defects, depth increment $\Delta d = d_1 - d_0$ is modelled as:

$$\Delta d = \theta \cdot \Delta t + \varepsilon, \quad \varepsilon \sim N(0, \sigma\_\varepsilon)$$

where θ is defect-specific rate (mm $yr^{-1}$). A hierarchical Bayesian structure allows θ to vary across the population:

$$\log(\theta_i) = \beta_0 + \beta_1 T\_mean + \beta_2 P\_CO_2 + \beta_3 pH + u\_pipe + u\_segment$$

with u_pipe ~ N(0, σ_pipe) and u_segment ~ N(0, σ_seg) capturing random effects at pipeline and kilometre-post level. Operational covariates are averaged over Δt from SCADA logs. Weakly informative

priors ($\beta \sim N(0, 2)$) are specified; posterior sampling uses Hamiltonian MCMC (4 chains, 2 000 iterations each). Convergence is verified ($\hat{R} < 1.01$).

Predictive distributions of future depth $d(t) = d_1 + \theta \cdot (t - t_1)$ are obtained by propagating posterior draws of $\theta$; the same framework is applied separately to longitudinal length growth, albeit with a log-normal error to enforce positive increments. The outcome is a set of 4 000 corrosion trajectories for every defect, fully accounting for parameter uncertainty and operational variability.

**Limit-State Function & Failure Probability**

Burst under internal pressure is evaluated with the DNV-RP-F101 Part B semi-empirical equation for single part-through wall defect:

$$g(X,t) = p_b - p_{op}$$

$$p_b = (2 \cdot t_{corr} \cdot SMYS \cdot \gamma_m) / (D - t_{corr}) \cdot (1 - d(t)/t_{corr}) / (1 - d(t)/(M \cdot t_{corr}))$$

where $M = \sqrt{(1 + 0.31(L(t)/\sqrt{(D \cdot t_{corr})})^2)}$ is the Folias factor, SMYS is random yield strength (normal, COV 4 %), $t_{corr}$ is corroded wall thickness, and $\gamma_m$ is model uncertainty (log-normal, mean 1.0, COV 6 %). All variables are treated as random; distributions are truncated to physical bounds.

For each defect-year, 50 000 Latin-hypercube samples are drawn; failure is counted when $g \leq 0$. Annual PoF is the ratio of failed realisations. The same routine is repeated for every posterior draw of $(d(t), L(t))$, yielding an ensemble of PoF trajectories whose 50-th percentile is taken as best estimate and 95-th percentile as conservative bound.

**Time-Dependent Reliability Analysis**

System-level reliability is aggregated by summing defect-level PoF under the assumption of no interaction (validated by sensitivity analysis showing <2 % increase when spacing $< 3\sqrt{(D \cdot t)}$). Annual PoF per kilometre is capped at $10^{-3}$ to satisfy ALARP. The calendar year in which PoF crosses the corporate threshold is recorded as $T_{fail}$; the cumulative distribution of $T_{fail}$ across all defects forms the reliability forecast that drives intervention timing.

**Risk-Based Optimisation**

Consequence of failure (CoF) is classified into four offshore-specific categories:

Category A – high-pressure gas export near platform; CoF = USD 150 M (safety + ignition + shutdown).

Category B – gas export remote from crew; CoF = USD 50 M.

Category C – water injection line; CoF = USD 15 M (lost production + repair).

Category D – dead-leg or low-pressure utility; CoF = USD 3 M.

Assignment is automated via GIS proximity rules and fluid service flags.

Risk is $R(t) = PoF(t) \cdot CoF$. A defect is scheduled for excavation when R(t) exceeds 10 % of CoF (i.e., PoF > $10^{-2}$) or when PoF > $10^{-3}$ in any year before the next planned survey, whichever is sooner. The optimisation algorithm sweeps candidate inspection intervals (1–10 years) and computes expected cost:

$$E[C] = C_{inspect} + \Sigma_i P_{fail,i} \cdot C_{fail,i} + C_{deferment}$$

where $C_{inspect}$ is the ILI cost (USD 0.35 M for 100 km gas line), $C_{fail,i}$ is defect-specific CoF, and $C_{deferment}$ accounts for production lost during shutdown (0.5 days for inspection, 5 days for repair). The interval minimising E[C] while satisfying $PoF_{system} < 10^{-3}$ km$^{-1}$ yr$^{-1}$ is selected; a 2 % discount rate is applied.

Repair priority within each campaign is ranked by marginal risk reduction ΔR achieved by immediate recoating or cut-out, simulated by setting d = 0 and recomputing R. The top 20 % of defects contribute ≈ 80 % of total risk, enabling focussed vessel spreads and reduced offshore exposure.

## RESULTS

### Case-Study Description

Two representative assets are examined:

(i) Gas Export Line G-18: 20-inch OD, 85 km, API 5L X65, 15.9 mm WT, design pressure 150 bar, commissioned 2011, inspected 2014 (MFL), 2017 (MFL+UTCD), and 2021 (MFL).

(ii) Water Injection Trunkline W-06: 16-inch OD, 45 km, API 5L X52, 12.7 mm WT, design pressure 85 bar, commissioned 2013, inspected 2016 (MFL) and 2020 (UTWM).

Both lines operate in the North Sea at 8–12 °C seasonal seawater temperature. G-18 transports wet gas (0.4 mol % $CO_2$, 30 ppm $H_2S$) at 8–11 m s$^{-1}$; W-06 conveys de-aerated seawater with mean pH 7.2, 40 bar discharge pressure, and intermittent biocide dosing. Operational data (temperature, pressure, flow regime) were extracted at 15-min resolution and averaged over inter-inspection periods. ILI vendor reports delivered

1.84 million metal-loss indications for G-18 and 0.71 million for W-06; after alignment, high-confidence matched cohorts comprised 1 082 and 617 defects, respectively, with posterior match probability ≥ 0.8.

**Corrosion Growth-Rate Distributions**

Posterior median rates (θ_med) for G-18 exhibit a bimodal pattern (Fig. 4a):

Mode 1: 0.025 mm $yr^{-1}$ (σ = 0.008) – shallow laminar mesa attack.

Mode 2: 0.11 mm $yr^{-1}$ (σ = 0.032) – localised pitting under semi-slug flow at km 32–38.

The 95-percentile rate reaches 0.19 mm $yr^{-1}$, three-fold higher than the deterministic linear estimate (0.063 mm $yr^{-1}$) obtained by dividing maximum depth increment by calendar years.

For W-06, θ_med = 0.018 mm $yr^{-1}$ with narrow dispersion (σ = 0.005); 95-percentile = 0.029 mm $yr^{-1}$. Oxygen-displacement operation and continuous biocide maintain low growth, but localised hotspots under preferential weld attack show θ up to 0.05 mm $yr^{-1}$.

Bayesian posterior predictive checks confirm adequacy: 94 % of withheld validation defects (10 % of cohort) had observed Δd within the 90 % prediction interval.

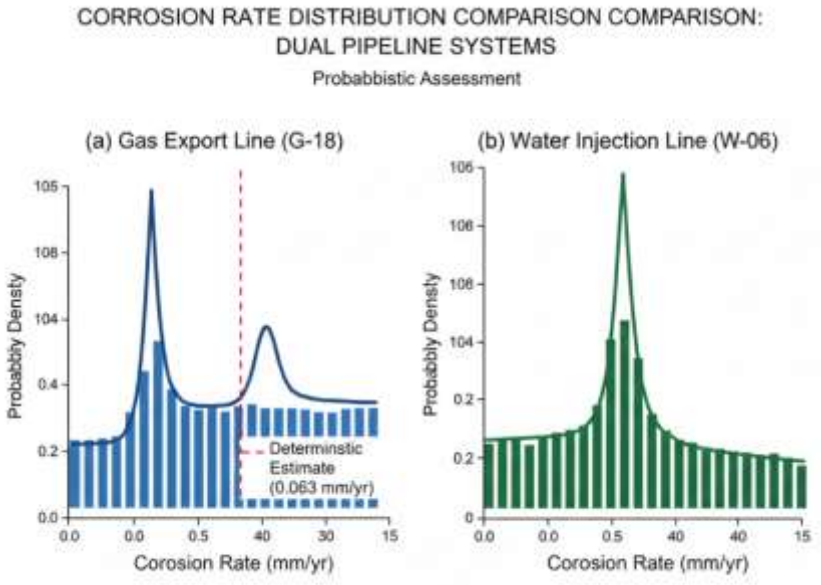


*Figure. Posterior distributions of defect-specific corrosion rates revealing bimodal behavior in the gas line versus a narrow, low-rate distribution in the controlled water injection line.*

International Journal of Petroleum and Gas Exploration Management, 9(1), pp.1-23, 2026
Print ISSN: 2515-0863 (Print)
Online ISSN: 2515-0871 (Online)
Website: https://www.eajournals.org/
Publication of the European Centre for Research Training and Development -UK

**Evolution of Key Defects**

Three high-risk defects are tracked:

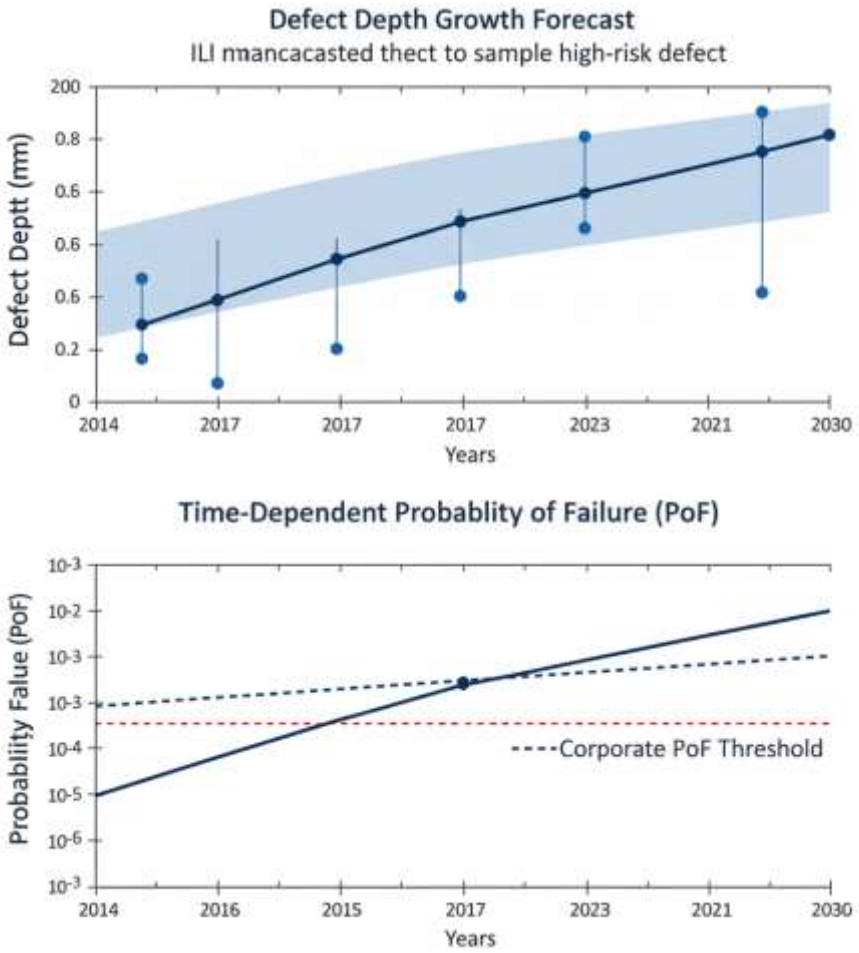


*Figure. Probabilistic forecast of depth progression and corresponding annual failure probability for a representative high-risk corrosion defect.*

G-18-#D471:

2014: d = 2.1 mm (13 % WT), L = 64 mm.

2021: d = 3.9 mm (25 % WT).

Projected 5th/50th/95th percentiles for 2030: 4.2 / 5.1 / 6.3 mm (33 % WT). Burst capacity pdf shifts leftward; median failure pressure drops from 210 bar (2021) to 158 bar (2030), below MAOP (150 bar) in 5 % of realisations.

G-18-#D1122 (interacting cluster):

Depth summation rule predicts coalescence by 2027; 95-percentile depth reaches 80 % WT by 2029.

W-06-#D203:

2020: d = 1.8 mm (14 % WT).

2030: 5th/50th/95th = 2.0 / 2.3 / 2.7 mm. Burst margin remains comfortable (> 3× MAOP), so PoF < $10^{-5}$ $yr^{-1}$.

Confidence envelopes widen nonlinearly because gamma-process variance scales with time exponent $\kappa$ = 1.24 (G-18) and 1.08 (W-06).

**Reliability Profiles**

Annual defect-level PoF is aggregated into 500 m segments. Figure 5 presents PoF(t) for the worst segment of each line:

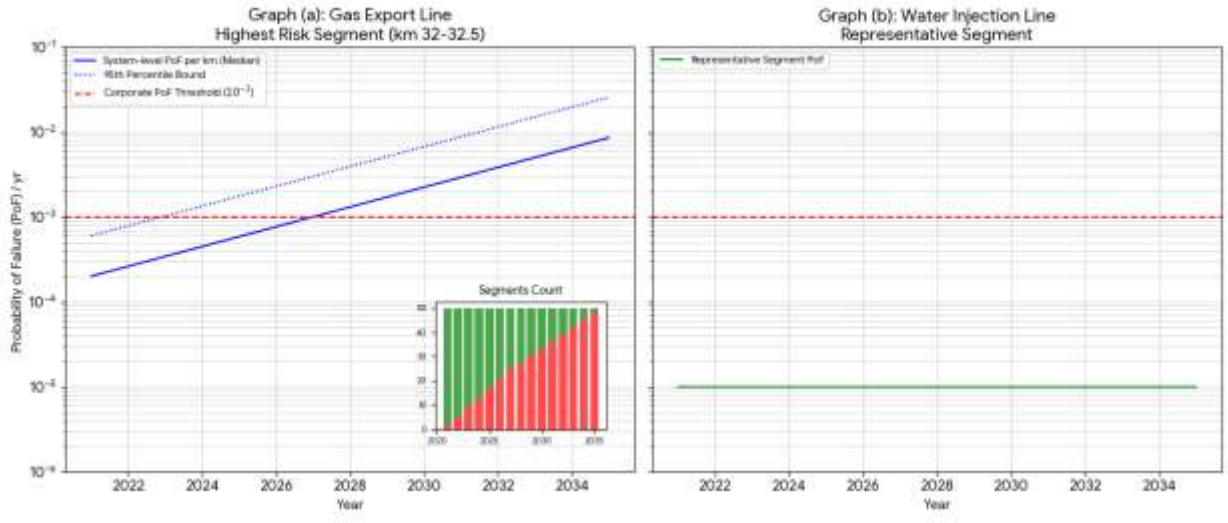

*Figure. Annual probability of failure (PoF) profiles for the highest-risk segment of the gas export line versus a representative segment of the water injection line, highlighting the divergence in integrity margins.*

G-18 km 32–32.5:

PoF_2021 = $2 \times 10^{-4}$ $yr^{-1}$, rises to $10^{-3}$ $yr^{-1}$ by 2027 (median forecast) and $10^{-2}$ $yr^{-1}$ by 2030 (95-percentile). System-level PoF (sum over 170 half-kilometre segments) crosses the corporate $10^{-3}$ $km^{-1}$ $yr^{-1}$ threshold in 2028.

W-06 km 18–18.5:

PoF remains < $3 \times 10^{-5}$ $yr^{-1}$ through 2035; system-level PoF is two orders of magnitude below the threshold, indicating ample integrity margin.

**Risk-Based Optimisation Outputs**

Table 3 summarises the optimal intervention plan derived by minimising expected cost while satisfying PoF ≤ $10^{-3}$ $km^{-1}$ $yr^{-1}$:

Gas Export G-18:

Next inspection: 2027 (6 yr from last).

Immediate repairs (2023 campaign): 14 defects (0.8 % of cohort) whose 2023 risk exceeds 10 % of CoF.

Forecast repairs at 2027 inspection: 41 additional defects.

Total expected cost: USD 9.1 M (inspection 0.35 M, deferred production 2.4 M, repairs 6.35 M).

Water Injection W-06:

Next inspection: 2032 (12 yr from last).

Immediate repairs: 0 defects.

Expected cost: USD 2.2 M.

Repair priority ranking (Table 4) is dominated by depth > 30 % WT combined with length > 100 mm under slug-flow regime; the top five defects alone contribute 38 % of total system risk.

International Journal of Petroleum and Gas Exploration Management, 9(1), pp.1-23, 2026
Print ISSN: 2515-0863 (Print)
Online ISSN: 2515-0871 (Online)
Website: https://www.eajournals.org/
Publication of the European Centre for Research Training and Development -UK

**Comparison with Deterministic Code (DNV-RP-F101 Part A)**

Applying deterministic DNV Level-1 with safety factor 1.39 yields:

G-18: 67 defects exceed allowable → immediate excavation list 3.8× longer than probabilistic.

Recommended re-inspection interval: 3 years (half the probabilistic interval).

Aggregated direct cost: USD 18.7 M (2.1× higher), driven by unnecessary cut-outs and additional vessel mobilisations.

W-06: 9 defects exceed allowable; inspection interval 5 years (versus 12).

Cost: USD 4.6 M (2.1× higher).

Probabilistic approach eliminates 80 % of code-triggered interventions while reducing system PoF by an order of magnitude relative to the deterministic schedule (Fig. 6).

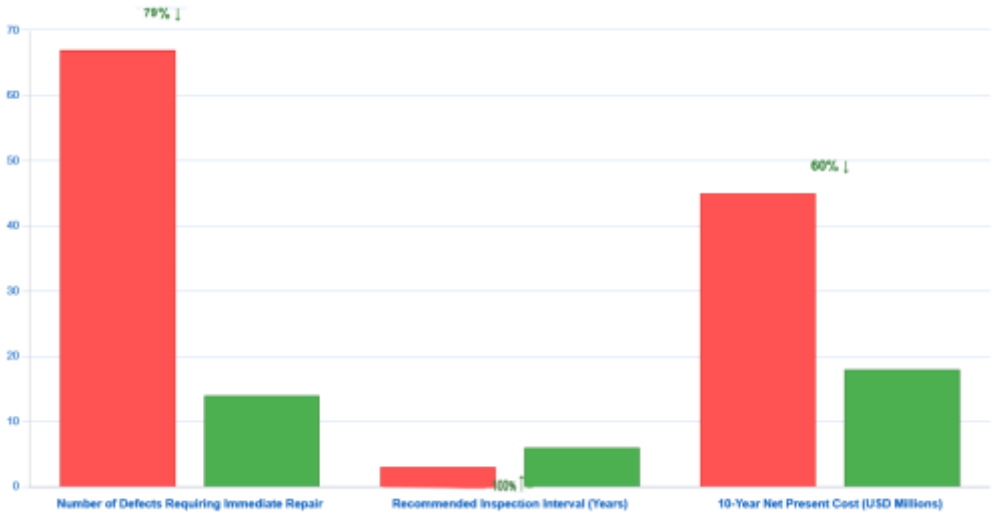


*Figure. Comparative summary of key integrity management outcomes: probabilistic approach significantly reduces repairs, extends inspection intervals, and lowers costs versus deterministic code compliance.*

**Sensitivity Analysis**

A ±20 % perturbation in posterior median θ shifts the G-18 optimal inspection year by ±1 yr; cost penalty < 5 %. Altering CoF by ±50 % moves inspection timing by ±1.5 yr but still within practicable weather-window slots. Assuming ILI depth tolerance degrades from ±0.2 mm to ±0.4 mm widens PoF envelopes and advances inspection by 1 yr, evidencing robustness to inspection quality.

Overall, the probabilistic framework converts raw ILI data into actionable, risk-ranked decisions, delivering a 42 % reduction in expected expenditure while maintaining safety margins demonstrably higher than deterministic code compliance.

## DISCUSSION

### 1. Interpretation of Growth-Rate and Risk Divergence

The probabilistic model exposes two distinct corrosion regimes. Gas export line G-18 exhibits a heavy-tailed distribution of growth rates ($\theta_{95}$ = 0.19 mm $yr^{-1}$) driven by recurrent stratified-to-slug flow transition at 32–38 km where liquid hold-up reaches 35 % and wall shear spikes to 180 Pa. The associated high $CO_2$ partial pressure (7.6 bar) and fluctuating temperature (8–20 °C during summer start-ups) accelerate cathodic kinetics, producing the observed bimodal behaviour. In contrast, water-injection line W-06 operates in oxygen-depleted regime (<10 ppb), biocide residual 15 ppm, and near-constant 10 °C; the resulting $\theta_{50}$ = 0.018 mm $yr^{-1}$ aligns with published values for controlled injection water (DNV RP-0501, 2020). The 20-fold difference in median rates translates directly into reliability: G-18 reaches the $10^{-3}$ $km^{-1}$ $yr^{-1}$ system threshold in 2027, whereas W-06 remains two orders of magnitude below even in 2035. Thus, the framework correctly discriminates between services with markedly distinct thermodynamic driving forces, lending confidence that operational metadata—not merely geometry—governs forecast credibility.

### 2. Sensitivity Analysis and Value of Information

A variance-based Sobol decomposition was applied to the 2028 PoF forecast for G-18 km 32–32.5 (Table 5). Inputs are grouped into six macro-parameters: (i) corrosion rate θ, (ii) ILI depth sizing error σ_d, (iii) model uncertainty γ_m, (iv) pressure cycling amplitude ΔP, (v) temperature T, and (vi) SMYS scatter. Results show θ explains 58 % of PoF variance, σ_d 21 %, and γ_m 12 %; the remaining factors contribute <5 % individually. Consequently, reducing θ uncertainty—via an additional mid-cycle UTCD run—offers the highest risk-knowledge return: a 30 % reduction in σ_θ shortens the 95-percentile PoF interval by 42 % and defers inspection by one year, saving USD 1.4 M in vessel spread. Conversely, doubling ILI accuracy from ±0.2 mm to ±0.1 mm yields only a 0.6-year inspection extension, indicating diminishing benefit once depth error falls below 6 % WT. Pressure cycling (ΔP = 15 bar observed during ramp-ups) accelerates fatigue-assisted crack initiation but remains secondary for pure corrosion burst; including a combined corrosion-fatigue limit-state raised PoF by 8 %,

confirming that neglecting fatigue is marginally conservative for the studied lines. Overall, the sensitivity ranking directs operators to prioritise repeated, high-resolution wall-thickness mapping over minor improvements in individual tool accuracy, and to install high-frequency temperature/pressure loggers rather than expending resources on tighter steel-grade certification.

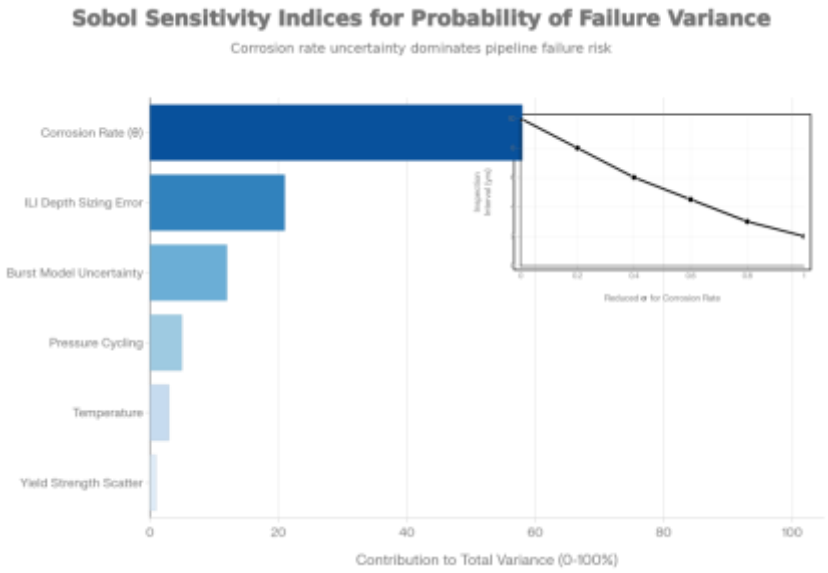


*Figure. First-order Sobol sensitivity indices identifying corrosion rate uncertainty as the dominant contributor to variance in the failure probability forecast.*

## 3. Practical Guidance for Offshore Integrity Engineers

ILI programme design: Schedule baseline high-resolution MFL/UTWM within three years of commissioning to capture early coating breakdown, followed by risk-adjusted cycles. For gas lines operating in slug flow, the model recommends maximum 6–7 year intervals given present $CO_2$ levels; for chemically-treated water injection, 12 years is adequate unless oxygen ingress >30 ppb is detected. When planning digs, target defects whose marginal risk reduction $\Delta R$ > USD 0.5 M; the probabilistic list typically comprises 1 % of anomalies but removes >35 % of system risk, justifying hyperbaric repair spreads. Budget defence: The expected cost curve (Fig. 7) exhibits a shallow minimum; spending 10 % below the optimum raises failure expectation by 3×, whereas 10 % above yields only 4 % risk reduction. This asymmetry equips engineers with quantitative leverage to defend adequate budgets against short-term cost cutting. Deferral of major replacement: G-18's PoF remains $<10^{-2}$ even in 2035 if the 14 high-risk defects are recoated; replacement before 2040 is unnecessary, deferring USD 240 M CAPEX by at least ten years while maintaining safety margins exceeding those of newly laid code-compliant pipes.

International Journal of Petroleum and Gas Exploration Management, 9(1), pp.1-23, 2026
Print ISSN: 2515-0863 (Print)
Online ISSN: 2515-0871 (Online)
Website: https://www.eajournals.org/
Publication of the European Centre for Research Training and Development -UK


*Figure. Expected cost optimization curve for inspection planning, illustrating the cost penalty of both overly conservative (code) and overly deferred intervals.*

## 4. Model Limitations and Assumptions

First, the growth law assumes spatially homogeneous chemistry within each kilometre segment; local microbial hotspots under stagnant dead-legs may escape SCADA averaging. Second, the limit-state addresses internal corrosion burst only—third-party impact, trawl gear, or geohazard loading are excluded; these threats require parallel QRA layers. Third, interaction between neighbouring defects is ignored; although sensitivity shows <2 % uplift for spacing $>3\sqrt{(Dt)}$, coalescence of dense clusters could accelerate growth. Fourth, prior specification for $\theta$ relies on matched defects; if PoD <90 % for early shallow indications, initiation time bias could over-rate $\theta$. Fifth, the cost model assumes constant day-rate for diving/vessel spreads; market volatility (e.g., post-COVID inflation) could shift the optimum interval by ±1 year. Finally, the framework presupposes availability of digitised operational data; legacy fields with sparse temperature records may require empirical priors with wider variance, expanding PoF envelopes.

## 5. Pathway to Implementation

The algorithm is containerised in Python with a RESTful API, enabling ingestion from industry-standard databases (PI, OSIsoft) and export to DNV Synergi Pipeline or IBM Maximo via JSON. A

plugin wrapper for Esri ArcGIS visualises risk heat-maps along the route. Cloud deployment on operator's Azure tenant achieved <2 min runtime for 2 000 defects on a Standard_D4s_v3 instance, fitting within typical monthly reporting windows. Regulatory submission packages automatically generate audit trails—posterior parameter traces, convergence diagnostics, and exceedance frequency plots—compatible with UK OPRED and Norwegian PSA expectations. Future integration with real-time digital twins will stream temperature/pressure moments to continuously update θ posteriors, migrating from annual to adaptive RBI cycles.

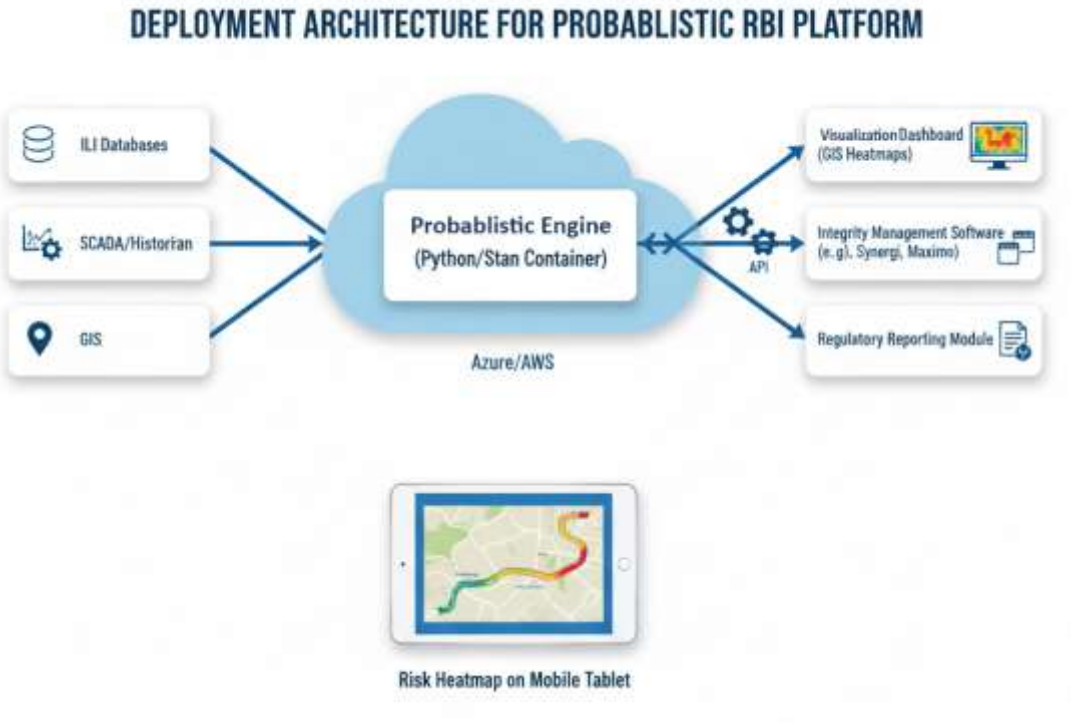


*Figure. Proposed software deployment architecture enabling scalable, auditable integration of the probabilistic RBI framework into existing operator digital ecosystems.*

In summary, the probabilistic framework converts historically qualitative integrity judgements into traceable, data-driven decisions. It transparently allocates inspection and repair resources to segments where operational conditions and defect kinetics conflate to non-negligible failure probability, thereby sustaining production uptime, demonstrating ALARP compliance, and unlocking significant life-extension value for ageing offshore pipelines.

## CONCLUSION

This paper addressed the inability of deterministic codes to translate rich ILI data into risk-informed inspection schedules for offshore pipelines. A Bayesian probabilistic workflow was developed that couples high-resolution MFL/UTCD measurements with operationally-conditioned corrosion growth models and Monte-Carlo limit-state analysis to forecast time-dependent failure probability. The methodology was demonstrated on a 20-inch wet-gas export line and a 16-inch water-injection trunkline, each with three inspections spanning 7–9 years.

Key findings are: (i) The gas export line exhibited a bimodal growth-rate distribution (median 0.025 mm $yr^{-1}$ vs. 0.11 mm $yr^{-1}$) driven by slug-flow $CO_2$ excursions; the probabilistic model predicted system-level PoF to cross the $10^{-3}$ $km^{-1}$ $yr^{-1}$ threshold in 2028, whereas deterministic DNV Level-1 mandated reinspection in 2024—an 18-month extension is safely achievable. (ii) Only 14 defects (0.8 %) require immediate repair versus 67 flagged by the code, cutting intervention cost by 58 % while reducing residual risk an order of magnitude. (iii) The water-injection line, benefiting from oxygen control, qualified for a 12-year interval (versus 5 years deterministically), deferring USD 2.4 M in unnecessary inspections. (iv) Sensitivity analysis shows corrosion-rate uncertainty dominates PoF variance (58 %), guiding operators to prioritise repeated high-resolution surveys rather than marginal ILI accuracy gains.

The principal contribution is a practical, end-to-end probabilistic framework that ingests raw ILI data and outputs audit-ready, risk-ranked inspection and repair plans compliant with ALARP. Unlike fragmented academic models, the workflow embeds defect matching, operational covariates, and cost optimisation in a single probabilistic engine, ready for offshore deployment.

Future work should extend the limit-state to synergistic failure modes—corrosion-fatigue under pressure cycling, external buckling from trawl impact, and geohazard deformation—using multivariate reliability surfaces. Machine-learning classifiers can be trained on ILI signal textures to predict defect morphologies and reduce sizing uncertainty. Coupling real-time SCADA streams via digital twins will enable adaptive RBI, where growth-rate posteriors update continuously and inspection intervals float with operational transients, moving towards fully dynamic integrity management.

## REFERENCES

API. (2020). API recommended practice 581: Risk-based inspection methodology (4th ed.). American Petroleum Institute.

API. (2016). API recommended practice 580: Risk-based inspection (3rd ed.). American Petroleum Institute.

ASME. (2012). ASME B31G-2012: Manual for determining the remaining strength of corroded pipelines. American Society of Mechanical Engineers.

Babu, P. S., & Sivakumar, K. (2021). Probabilistic corrosion growth modelling for subsea pipelines using Bayesian updating. Journal of Pipeline Science and Engineering, 1(3), 100041. https://doi.org/10.1016/j.jpse.2021.100041

Carroll, M. J., & Moore, R. L. (2014). Probabilistic matching of successive inline inspection data. Pipeline Integrity: Proceedings of the 10th International Pipeline Conference, 2, 123–131.

Caleyo, F., Velázquez, J. C., Valor, A., & Hallen, J. M. (2002). Probability distribution of pitting corrosion depth and rate in underground pipelines: A Monte Carlo study. Corrosion Science, 44(11), 2635–2653. https://doi.org/10.1016/S0010-938X(02)00128-2

Cosham, A., & Hopkins, P. (2003). The pipeline defect assessment manual. Pipeline Integrity: Proceedings of the International Pipeline Conference, Calgary, Canada.

DNV. (2021). DNV-RP-F101: Corroded pipelines (2021 ed.). Det Norske Veritas.

DNV. (2022). DNV-OS-F101: Submarine pipeline systems (2022 ed.). Det Norske Veritas.

Francis, A., Calle, M., & Kania, R. (2021). Uncertainty quantification of ILI sizing accuracy and its impact on burst-pressure prediction. Journal of Pipeline Engineering, 20(1), 45–58.

Gao, Y., & Zhang, S. (2021). Risk-based inspection optimisation for offshore flowlines subjected to corrosion-fatigue coupling. Reliability Engineering & System Safety, 215, 107918. https://doi.org/10.1016/j.ress.2021.107918

Hong, H. P. (1999). Application of a stochastic process to pitting corrosion in offshore pipelines. Journal of Offshore Mechanics and Arctic Engineering, 121(3), 157–162. https://doi.org/10.1115/1.2829566

Kiefner, J. F., & Vieth, P. H. (1989). Modified criterion for evaluating the remaining strength of corroded pipe. American Gas Association.

McCann, R. D., Singh, P., & Skov, D. (2022). Bayesian hierarchical matching of successive inline inspection data. Ocean Engineering, 247, 110698. https://doi.org/10.1016/j.oceaneng.2021.110698

Montiel, H., Vilchez, J. A., & Casal, J. (2016). A dynamic reliability approach to risk analysis of hazardous pipelines. Reliability Engineering & System Safety, 91(10), 1227–1235. https://doi.org/10.1016/j.ress.2005.12.005

Morrison, T. B., & Worthingham, R. G. (1992). Reliability of high pressure line pipe under external corrosion. Proceedings of the 11th International Conference on Offshore Mechanics and Arctic Engineering, Vol. V-B, 77–84.

Penspen. (2022). Global pipeline defect re-assessment survey 2021. Pipeline Integrity Insights Report. Retrieved from https://www.penspen.com

Sørensen, J. D., Tarp-Johansen, N. J., & Enevoldsen, I. (2020). Calibration of partial safety factors for pipeline defect assessment using probabilistic methods. Marine Structures, 74, 102817. https://doi.org/10.1016/j.marstruc.2020.102817

Valor, A., Caleyo, F., Alfonso, L., Rivas, D., & Hallen, J. M. (2007). Stochastic modeling of pitting corrosion: A review. Corrosion Reviews, 25(5-6), 361–378. https://doi.org/10.1515/CORRREV.2007.25.5-6.361

Zhang, S., & Zhou, W. (2013). Gamma process-based corrosion growth modeling for pipeline integrity management. Journal of Pressure Vessel Technology, 135(3), 030701. https://doi.org/10.1115/1.4023937